# Quantum State Engineering with Circuit Electromechanical Three-Body Interactions

Mehdi Abdi,[1] Matthias Pernpeintner,[1,2,3] Rudolf Gross,[1,2,3] Hans Huebl,[2,3] and Michael J. Hartmann[4]
[1]*Physik Department, Technische Universität München, James-Franck-Straße, 85748 Garching, Germany*
[2]*Walther-Meißner-Institut, Bayerische Akademie der Wissenschaften, Walther-Meißner-Straße 8, 85748 Garching, Germany*
[3]*Nanosystems Initiative Munich, Schellingstraße 4, 80799 München, Germany*
[4]*Institute of Photonics and Quantum Sciences, Heriot-Watt University, Edinburgh EH14 4AS, United Kingdom*
(Received 18 February 2015; published 28 April 2015)

We propose a hybrid system with quantum mechanical three-body interactions between photons, phonons, and qubit excitations. These interactions take place in a circuit quantum electrodynamical architecture with a superconducting microwave resonator coupled to a transmon qubit whose shunt capacitance is free to mechanically oscillate. We show that this system design features a three-mode polariton-mechanical mode and a nonlinear transmon-mechanical mode interaction in the strong coupling regime. Together with the strong resonator-transmon interaction, these properties provide intriguing opportunities for manipulations of this hybrid quantum system. We show, in particular, the feasibility of cooling the mechanical motion down to its ground state and preparing various nonclassical states including mechanical Fock and cat states and hybrid tripartite entangled states.

DOI: 10.1103/PhysRevLett.114.173602 PACS numbers: 42.50.Wk, 42.50.Dv, 85.25.-j, 85.85.+j

The quantum control of macroscopic objects is of great fundamental importance [1], and massive mechanical resonators strongly interacting with well-controlled quantum systems, e.g., photons and atomic excitations, are desired candidates for this purpose [2–4]. These can be employed for preparing nonclassical states in mechanical resonators [5–9] but are also of technological interest, e.g., for weak force sensing [10] and transduction of quantum information in quantum networks [11]. Particularly, nonlinear quantum phenomena are very desirable for the above purposes as they considerably extend the options for manipulation and control of quantum systems. Introducing an anharmonic part into a setup can, for example, strengthen its couplings and enrich its physics via the nonlinearities [12–16]. Here, we propose a circuit electromechanical hybrid architecture that combines a nanomechanical degree of freedom with both an intrinsically nonlinear component in the form of a superconducting qubit and nonlinear interactions between the mechanical mode, the qubit excitations, and a harmonic mode of an electrical resonator. As a key novelty, this architecture features three-body interactions between the mechanical and two electrodynamical degrees of freedom, which can not be approximated by effective two-body interactions due to the involved nonlinearities.

We explore a circuit quantum electrodynamical system consisting of a transmon qubit strongly coupled to a superconducting microwave resonator. In addition, the resonator-transmon system interacts with a nanomechanical oscillator. The advantage of a transmon is its robustness against fluctuations of background charges achieved by increasing the ratio of Josephson and charging energies $E_J/E_C$ [17] at the cost of a reduced anharmonicity. Nonetheless, its nonlinearity can still be exploited for controllably producing single photons in a superconducting transmission line resonator via excitation exchange [18] or for controllably producing propagating surface acoustic phonons [19]. Moreover, Josephson junctions integrated into a circuit electromechanical device can enhance its optomechanical couplings [15,20–22].

Here, we propose to couple the transmon-cavity system to a mechanical resonator by replacing one of the transmon's shunt capacitor legs with an oscillating nanobeam; see Fig. 1. Hereby, we introduce a nonlinear coupling between the qubit and the mechanical resonator that can reach the strong coupling regime; i.e., the bare coupling rate can exceed the relaxation rates of the system. In particular, as the nanomechanical transmon is embedded in a microwave cavity the hybrid system features an electromechanical three-body interaction with a flux tunable coupling rate. To show some assets of the system, we exploit these couplings and the anharmonicity of the transmon qubit to cool down the system to its ground state and prepare it in nonclassical states such as mechanical Fock and Schrödinger cat states.

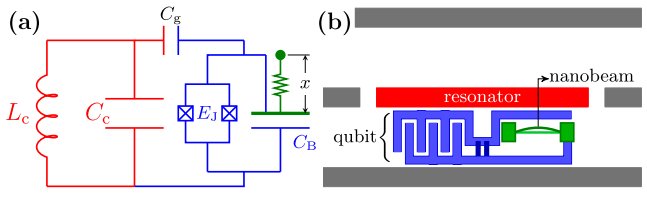


FIG. 1 (color online). (a) Circuit diagram and (b) sketch of the hybrid system composed of a transmon qubit, a superconducting coplanar waveguide resonator, and a mechanical oscillator.

 

*The model.*—Our system is composed of a superconducting coplanar waveguide resonator equivalent to an $L_cC_c$ oscillator, capacitively coupled to a transmon qubit via a gate capacitance $C_g$. The shunt capacitance $C_B$ of the transmon qubit depends on the position of a mechanical resonator as depicted in Fig. 1(b). The Hamiltonian of the complete system can be written as ($\hbar = 1$) (see the Supplemental Material [23])

$$\begin{aligned}\hat{H} &= \hat{H}_0 + \hat{H}_1 + \hat{H}_d,\\ \hat{H}_0 &= \omega_t \hat{a}^\dagger \hat{a} - \lambda(\hat{a}^\dagger)^2\hat{a}^2 + \Omega_m \hat{b}^\dagger \hat{b} + \omega_c \hat{c}^\dagger \hat{c} + i\chi(\hat{a}\hat{c}^\dagger - \hat{a}^\dagger \hat{c}),\\ \hat{H}_1 &= [g_t \hat{a}^\dagger \hat{a} + i g_{tc}(\hat{a}\hat{c}^\dagger - \hat{a}^\dagger \hat{c})](\hat{b} + \hat{b}^\dagger),\\ \hat{H}_d &= \mathcal{E}_L(\hat{c}e^{i\omega_L t} + \hat{c}^\dagger e^{-i\omega_L t}).\end{aligned} \tag{1}$$

Here, $\omega_t = E_C(\sqrt{8\zeta} - 1)$ with $\zeta = E_J/E_C$ is the transition frequency between the ground and the first excited state of the transmon, which is modeled as an anharmonic oscillator with annihilation (creation) operator $\hat{a}$ ($\hat{a}^\dagger$) and Duffing nonlinearity $\lambda = E_C/2$. The charging energy of the qubit is $E_C = e^2/2C_\Sigma$ with $C_\Sigma = C_g + C_B + C_J$ ($C_J$ is the capacitance of the Josephson junction). The nanomechanical resonator with natural frequency $\Omega_m$ is described by phononic operators $\hat{b}$ ($\hat{b}^\dagger$), and its displacement is given by $\hat{x} = x_{\mathrm{zpm}}(\hat{b} + \hat{b}^\dagger)$, where $x_{\mathrm{zpm}} = \sqrt{\hbar/2m\Omega_m}$ is its zero-point motion amplitude and $m$ its effective mass. The microwave cavity oscillates with frequency $\omega_c$ and is characterized by the bosonic mode operators $\hat{c}$ and $\hat{c}^\dagger$. An external microwave field drives the cavity with amplitude $\mathcal{E}_L$. The rate at which the qubit couples to the transmission line is $\chi = 4E_C n_{\mathrm{ac}}(\zeta/2)^{1/4}$ with $n_{\mathrm{ac}}$ the rms number of cavity-induced Cooper pairs. Moreover, the interactions between the mechanical resonator and the other parts of the system are quantified by the coupling rates $g_t = g_0\sqrt{2\zeta}$ for the transmon-mechanical mode interaction and $g_{tc} = 4g_0 n_{\mathrm{ac}}(\zeta/2)^{1/4}$ for the three-body electromechanical mode interaction, where $g_0$ is the bare coupling constant (Supplemental Material [23]). Notably, both couplings are enhanced as the ratio $E_J/E_C$ increases, which can be tuned *in situ* and in addition has the beneficial effect of enhancing the coherence time of the transmon. Finally, we mention that a rotating wave approximation (RWA) is applied to get the Hamiltonian $\hat{H}$. This is valid for $\zeta \gg 1$ and $\chi, g_t, g_{tc} \ll \omega_t, \omega_c$, which is compatible with the operation regime of our hybrid system.

In addition to the coherent evolution described by the above Hamiltonian, the system is affected by dissipation. The energy relaxation rate of the transmon is $\gamma_t = 1/T_1$, and its total dephasing rate is $1/T_2^* = 1/(2T_1) + 1/T_\phi$ where $\gamma_\phi = 1/T_\phi$ is the pure dephasing rate. High-quality superconducting qubits can be fabricated with relaxation and dephasing times as high as $T_1 \approx 50\ \mu$s and $T_2^* \approx 20\ \mu$s [24]. Yet, even higher values, $T_1 \approx 70\ \mu$s and $T_2^* \approx 90\ \mu$s, have been realized for three-dimensional cavity setups [25,26]. In addition, the microwave photons of the cavity are subject to loss at a decay rate of $\kappa_c$, and the mechanical resonator is coupled to a thermal bath with the rate $\Gamma_m = \Omega_m/Q_m$, where $Q_m$ is its mechanical quality factor. These dissipation processes are captured by a Liouvillian in Lindblad form. Thus, the full dynamics of our system is described by the master equation

$$\begin{aligned}\dot{\rho} = &-i[\hat{H}, \rho] + \gamma_t \mathcal{D}_{\hat{a}}\rho + \gamma_\phi \mathcal{D}_{\hat{a}^\dagger\hat{a}}\rho + (\bar{n}+1)\Gamma_m \mathcal{D}_{\hat{b}}\rho\\ &+ \bar{n}\Gamma_m \mathcal{D}_{\hat{b}^\dagger}\rho + \kappa_c \mathcal{D}_{\hat{c}}\rho,\end{aligned} \tag{2}$$

where $\mathcal{D}_{\hat{o}}\rho = \hat{o}\rho\hat{o}^\dagger - (\hat{o}^\dagger\hat{o}\rho + \rho\hat{o}^\dagger\hat{o})/2$ is the dissipator and $\bar{n} = \{\exp[(\hbar\Omega_m)/(k_B T)] - 1\}^{-1}$ is the thermal phonon number.

*Polariton-mechanical mode interaction.*—For typical configurations, the transmon-cavity interaction is in the strong coupling regime ($\chi \gg \gamma_t, \kappa_c$). It is therefore convenient to describe the subsystem of cavity photons and qubit excitations in terms of dressed state excitations called polaritons, which decouple the interaction $i\chi(\hat{a}\hat{c}^\dagger - \hat{a}^\dagger\hat{c})$. In terms of these *polaritonic* modes $\hat{p}_\pm = \alpha_\pm \hat{a} \mp i\alpha_\mp \hat{c}$ (the explicit forms of $\alpha_\pm$ are given in the Supplemental Material [23]), the Hamiltonian (1) reads

$$\hat{H}_0 = \sum_{k=\pm}[\omega_k \hat{p}_k^\dagger \hat{p}_k - \lambda_k(\hat{p}_k^\dagger)^2\hat{p}_k^2] + \hat{H}_{+-} + \Omega_m \hat{b}^\dagger \hat{b}, \tag{3a}$$

$$\hat{H}_1 = \left[\sum_{k=\pm} g_k \hat{p}_k^\dagger \hat{p}_k + G(\hat{p}_+^\dagger \hat{p}_- + \hat{p}_+ \hat{p}_-^\dagger)\right](\hat{b} + \hat{b}^\dagger), \tag{3b}$$

where the polariton resonances are given by $\omega_\pm = \alpha_\pm^2\omega_t + \alpha_\mp^2\omega_c \pm 2\alpha_+\alpha_-\chi$, while the polariton-mechanical mode coupling rates are $g_\pm = \alpha_\pm^2 g_t + 2\alpha_+\alpha_- g_{tc}$ and $G = \alpha_+\alpha_- g_{\mathrm{t}} + (\alpha_+^2 - \alpha_-^2)g_{tc}$, and the nonlinearity for each polariton is $\lambda_\pm = \alpha_\pm^4\lambda$ (Note that $G > g_{tc}$ due to the contribution from $g_t$). There are thus three-body interactions for which the nonlinearity $\lambda$ precludes the linearization of the terms $\hat{p}_+^\dagger\hat{p}_-$ or $\hat{p}_+\hat{p}_-^\dagger$. This is in contrast to the original three-mode interaction with strength $g_{tc}$ or to optomechanical couplings in standard settings [27]. We have included all the interpolariton interaction terms in $\hat{H}_{+-}$; see the Supplemental Material [23]. Note that except for an intensity-intensity interaction, all these interpolariton interactions can be neglected in a RWA (Supplemental Material [23]) provided $\omega_+ - \omega_- = [\Delta^2 + 4\chi^2]^{1/2} \gg \lambda$, where $\Delta = \omega_t - \omega_c$ is the detuning between the transmon and cavity frequencies. This condition calls for a large photon-qubit coupling rate ($\chi \gg \lambda$) and/or large transmon-cavity detuning ($\Delta \gg \lambda$). To ensure the validity of the above RWA, we work in the off-resonance regime with $\Delta \gg \lambda$. The polariton-mechanical interactions in Eq. (3b) provide us with a toolbox for the quantum control of the state of the mechanical resonator, which is our main interest for the proposed architecture in this Letter.

*Cooling the mechanical resonator.*—A first question of interest is whether our setup allows for ground-state

cooling of the mechanical mode, as this is a prerequisite for many state preparation protocols. We show that this is indeed feasible using sideband cooling [28]. In principle, both interactions of Eq. (3b) are capable of performing the task. For the three-mode interaction, one would transfer a mechanical phonon and a lower polariton excitation into a higher polariton excitation $\omega_- + \Omega_m = \omega_+$, which subsequently decays. However, a simpler and more efficient route is to use the couplings $\hat{p}_\pm^\dagger \hat{p}_\pm (\hat{b} + \hat{b}^\dagger)$ at large cavity–transmon detunings. Here, one polariton is dominantly photonlike, while the other describes mainly a transmon excitation. In this regime, the photonlike polariton is practically decoupled from the mechanical mode, while the transmonlike polariton strongly interacts with it at a coupling rate close to $g_t$. For this kind of interaction, the final occupation number of the mechanical mode is limited by the total dephasing time $T_2^*$ of the qubit, and the ground state can be reached for $\Omega_m T_2^* > 1$ [29].

We numerically solve Eq. (2) with the Hamiltonian of Eq. (1) for two different sets of parameters. Set No. 1: $\zeta_c = 150$ [the resonance value, i.e., $\omega_t(\zeta_c) = \omega_c$], $m = 1$ pg, $g_0/2\pi = 2.9$ kHz, $\Omega_m/2\pi = 10$ MHz, $\kappa_c/2\pi = 10$ kHz, $\gamma_t/2\pi = 3$ kHz, and $n_{\rm ac} = 8.5 \times 10^{-4}$. Set No. 2: $\zeta_c = 142$, $m = 3$ pg, $g_0/2\pi = 3.3$ kHz, $\Omega_m/2\pi = 1$ MHz, $\kappa_c/2\pi = 50$ kHz, $\gamma_t/2\pi = 5$ kHz, and $n_{\rm ac} = 1.4 \times 10^{-2}$. We also take $\gamma_\phi = 2\gamma_t$ and use the common parameters $E_C/2\pi = 0.5$ GHz, $\omega_c/2\pi \approx 17$ GHz, and $Q_m = 10^6$. The considered mechanical parameters are compatible with experimental reported values [30–32]. In Fig. 2 we plot the numerical results for the final phonon numbers achievable by cooling via either of the polaritons. We find that it is possible to cool the mechanical resonator from $\bar{n} \approx 20$ phonons (corresponding to an ambient temperature $T \simeq 10$ mK) to $\bar{n}_f \approx 0.12$ for the parameter set No. 1 and from $\bar{n} \approx 100$ phonons (environment temperature $T \simeq 5$ mK) to $\bar{n}_f \approx 0.03$ for the parameter set No. 2. The multiple cooling resonances apparent in Fig. 2(b) are a signature of the nonlinearity of the coupling [33] and, thus, provide a measurable witness for the nonlinearity of the transmon-vibrational mode interaction. Having shown the feasibility of ground-state cooling, we now describe two state preparation protocols enabled by our device.

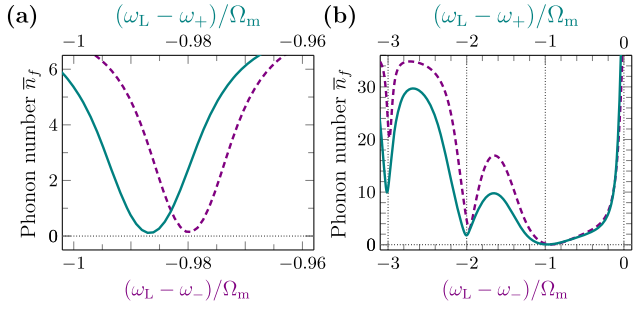


FIG. 2 (color online). Mechanical final phonon numbers versus drive detuning when only one of the polaritons $\hat{p}_+$ (solid lines) or $\hat{p}_-$ (dashed lines) is driven: (a) parameter set No. 1 with $\zeta = 150 \pm 50$ and (b) parameter set No. 2 with $\zeta = 142 \pm 60$.

*Mechanical Fock states.*—We first describe a protocol for preparing the mechanical resonator in Fock states. Our strategy here is to first generate individual polaritonic excitations and then transfer them to the mechanics via the three-mode interaction in Eq. (3b). To this end, sideband cooling first brings the mechanical resonator close to its ground state. Properly shaped microwave pulses at suitable frequencies can generate single-qubit rotations for the polaritons [34]. Hence, the polariton with higher frequency is excited by such a pulse. Then the transmon is tuned to the point where $\omega_+ - \omega_- = \Omega_m$, and the system evolves for a time $\tau_1 = \pi/2G$, which converts the higher-energy polariton into a lower-energy polariton and a single phonon in the mechanical resonator. The generated lower-energy polariton is finally annihilated by another microwave pulse, leaving the system in a single phonon Fock state.

Strong three-body interactions and hence fast excitation transfer could of course be achieved for $\omega_t \approx \omega_c$ (Supplemental Material [23]). Yet, in this regime all polariton-mechanical interactions have the same strength $g_+ = g_- = G \approx g_t/2$, which enables additional undesirable transfer channels that hamper the protocol. Hence, we demand for sufficiently large mechanical frequencies to suppress these unwanted interactions via a RWA and simultaneously ensure $\omega_+ - \omega_- = \Omega_m$. At the same level of accuracy, the three-mode interaction becomes $G(\hat{p}_+^\dagger \hat{p}_- \hat{b} + \hat{p}_+ \hat{p}_-^\dagger \hat{b}^\dagger)$. Furthermore, the transfer process must be much faster than the decoherence rates of the system; therefore, the restrictions on the system are $\max\{\gamma_t, \tilde{\Gamma}_m\} \ll g_t \ll \Omega_m$, where $\tilde{\Gamma}_m \approx \bar{n}\Gamma_m$ is the effective mechanical decoherence rate. The parameter set No. 1 satisfies the above criteria.

To provide evidence for its feasibility, we numerically simulate the protocol, including the initial cooling to the ground state, by solving the full master equation (2). As very high fidelities for single-qubit gates have already been demonstrated, we neglect errors in the polariton excitation and deexcitation steps. The fidelity for a single-phonon state prepared by sideband cooling followed by the above protocol reaches 70% for the parameter set No. 1 (see Fig. 3) and could even be enhanced further by increasing the coupling rate and/or starting from better ground states, e.g., by employing qubit reset methods [35]. To achieve higher number states, the process can be repeated until the target state is reached, where the interaction times for the swap need to be adjusted to $\tau_n = \pi/2\sqrt{n}G$ with $n$ being the number of mechanical phonons that will be obtained at the end of each stage. Note that although the interpolariton interactions are considerable, they will not play a role in this process as long as the total number of polaritons does not exceed unity (Supplemental Material [23]). Once prepared, the state of the mechanical resonator can be analyzed by adapting the measurement scheme pioneered in Ref. [18], i.e., tuning the transmon to the point where $\omega_+ - \omega_- = \Omega_m$ for various interaction times and reading out its excitation probability.

We note that the existence of the cavity mode is crucial for the above protocol since the qubit-mechanical

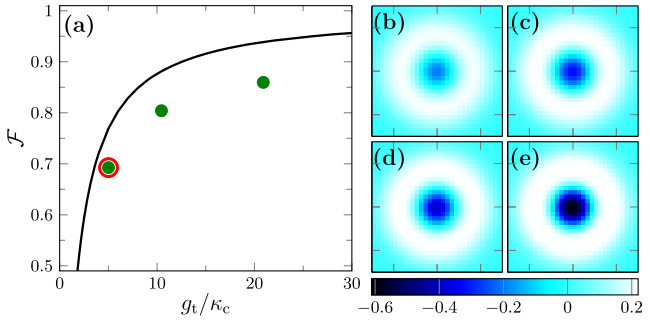


FIG. 3 (color online). (a) Fidelity of prepared single phonon state as a function of the transmon-mechanical coupling rate; for ideal initial ground state (solid line) and attainable ground state (dots). The point marked by the red circle corresponds to the parameter set No. 1. [(b)–(e)] Wigner quasiprobability distribution of the prepared Fock states with $g_t/\kappa_c \approx$ (b) 5, (c) 10, and (d) 21. (e) Ideal single phonon state, for comparison.

interaction is not in the form of a state transfer Hamiltonian, nor can it be changed to such form by intensely driving the (anharmonic) qubit, and the original three-mode interaction is not strong enough to be used in this way. Yet, the strong coupling of the cavity to the qubit generates a strong state transfer interaction of three-body form between the two polaritons on the one hand and the mechanical resonator on the other hand.

*Tripartite hybrid entanglement.*—We now turn to propose a protocol for preparing a non-Gaussian tripartite entanglement between qubit, cavity, and the mechanical resonator in our system. Such states are of interest from both fundamental and technical points of view [36]. In order to describe the steps for creating them, we go back to the original (not dressed) picture of the system and consider an effective three-level model for the transmon with ground state $|0\rangle_t$ and excited states $|1\rangle_t$ and $|2\rangle_t$.

The mechanical resonator is first cooled to its ground state with the transmon and cavity off resonance. By the application of a $[\pi/2]_{0\leftrightarrow 1}$ pulse, the qubit is prepared in a symmetric superposition of ground and first excited state. Then we let the mechanical resonator interact with the qubit. As the force exerted on the nanobeam depends on the state of the transmon, such an interaction results in a conditional displacement of the mechanical system from the origin of the phase space. The maximal amount of displacement is $2g_t/\Omega_m$, which is achieved when the interaction duration equals half the mechanical oscillation period. However, to have two distinguishable peaks in the mechanical phase space one needs $g_t \gtrsim \Omega_m$, which is not the case in our system. This hurdle can be circumvented by applying a sequence of $N_p$ regularly spaced $[\pi]_{0\leftrightarrow 1}$ pulses to the qubit with time intervals equal to half of the mechanical period. By choosing an odd number of pulses $N_p$, apart from an irrelevant global phase factor, one arrives at $\frac{1}{\sqrt{2}}(|0\rangle_t|0\rangle_c|\beta\rangle_m + |1\rangle_t|0\rangle_c|-\beta\rangle_m)$ with $\beta = (N_p+1)g_t/\Omega_m$ [37,38]. In the next step, the mechanical resonator can be turned into a superposition of odd and even cat states by applying a $[\pi/2]_{0\leftrightarrow 1}$ pulse to the transmon: $|\Psi_{tm}\rangle = \frac{1}{2}(|0\rangle_t|0\rangle_c|\psi_+\rangle_m + |1\rangle_t|0\rangle_c|\psi_-\rangle_m)$, which is already a bipartite qubit-mechanical entangled state. Here, $\mathcal{N}_\pm|\psi_\pm\rangle = \mathcal{N}_\pm(|\beta\rangle \pm |-\beta\rangle)$ with the normalization factor $\mathcal{N}_\pm = [2 \pm 2e^{-2|\beta|^2}]^{-1/2}$ is an even-odd cat state. Now, a single photon in the cavity can be conditionally produced via a $[\pi]_{1\leftrightarrow 2}$ pulse that flips the qubit from its first to its second excited state $|1\rangle_t \rightarrow |2\rangle_t$. Then a flux pulse of duration $\pi/2\sqrt{2}\chi$ sets this transmon transition in resonance with the cavity. Therefore, the second qubit excitation is transferred into the cavity, leading to

$$|\Psi_{tmc}\rangle = \frac{1}{2}(|0\rangle_t|0\rangle_c|\psi_+\rangle_m + |1\rangle_t|1\rangle_c|\psi_-\rangle_m). \quad (4)$$

The state of Eq. (4) is a hybrid Greenberger-Horne-Zeilinger state [39]. Evidently, $|\Psi_{tmc}\rangle$ could also be reduced to either even or odd cat states of the mechanical mode by performing a postselection based on the readout of the qubit or cavity state.

To attain macroscopically distinguishable mechanical cat states, a minimum number of pulses $N_p$ is required. On the other hand, the realizable $N_p$ is limited by the decoherence rates of the system. Thus, the parameter regime allowing for a successful preparation of the state (4) is $\pi \times \max\{\gamma_t, \tilde{\Gamma}_m\} < \Omega_m/N_p < g_t$. Note also that employing the third level for cloning the qubit excitations as cavity photons is necessary to get the state of Eq. (4). Furthermore, it is desirable to transfer the qubit second excitations into the cavity fast enough to decrease the unwanted displacements, so we also demand $\chi \gg \Omega_m$. Since we need to work with the transmon-mechanical mode interaction, we chose off resonance as the appropriate working regime, where the three-mode interaction is negligible.

In Fig. 4(a) the fidelity of the prepared odd cat state is plotted versus the number of applied pulses. Signatures of its generation can be obtained via extracting phonon

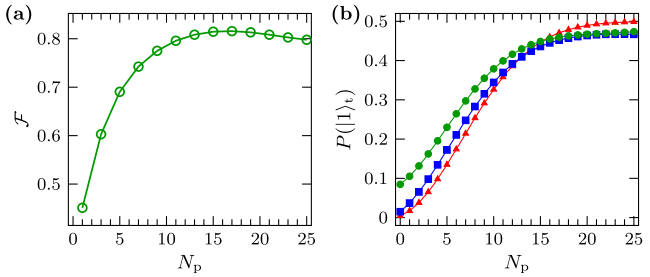


FIG. 4 (color online). (a) Fidelity of the prepared odd cat state versus $N_p$. (b) Probability of finding the transmon in its first excited state for the target state $|\Psi_{tmc}\rangle$ (red triangles), for the state resulting from a simulation starting from the ideal ground state (blue squares), and a simulation starting from an attainable ground state (green circles). The parameter set No. 2 is used in these simulations.

number probabilities with the method exploited in Ref. [40]. The protocol itself can be verified in an easier way by measuring the probability of finding the qubit in its first excited state or detecting a single photon in the output of the cavity as a function of the number of pulses $N_p$ applied to the qubit. Theoretically, for the ideal state $|\Psi_{tmc}\rangle$ these probabilities are $P(|1\rangle_t) = P(|1\rangle_c) = \frac{1}{2}(1 - \exp\{-2(N_p+1)^2 g_t^2/\Omega_m^2\})$. Figure 4(b) shows $P(|1\rangle_t)$ and the probability of finding the transmon in its first excited state (or detecting a single photon) for the states resulting from numerical simulations of the preparation protocol neglecting errors in single-qubit gate operations. The coincidence of the simulations with the theoretical ideal curve confirms the feasibility of the protocol.

M. A. acknowledges support by the Alexander von Humboldt Foundation via a postdoctoral fellowship, H. H. and R. G. by the German Research Foundation (DFG) via the SFB 631, and M. J. H. by the DFG via HA 5593/3-1 and the SFB 631.

[1] A. O. Caldeira and A. J. Leggett, Phys. Rev. Lett. **46**, 211 (1981).
[2] C. Monroe, D. M. Meekhof, B. E. King, and D. J. Wineland, Science **272**, 1131 (1996).
[3] S. Mancini, V. I. Man'ko, and P. Tombesi, Phys. Rev. A **55**, 3042 (1997).
[4] R. G. Knobel and A. N. Cleland, Nature (London) **424**, 291 (2003).
[5] A. D. Armour, M. P. Blencowe, and K. C. Schwab, Phys. Rev. Lett. **88**, 148301 (2002).
[6] W. Marshall, C. Simon, R. Penrose, and D. Bouwmeester, Phys. Rev. Lett. **91**, 130401 (2003).
[7] M. Abdi, S. Pirandola, P. Tombesi, and D. Vitali, Phys. Rev. Lett. **109**, 143601 (2012).
[8] S. Rips, M. Kiffner, I. Wilson-Rae, and M. J. Hartmann, New J. Phys. **14**, 023042 (2012).
[9] S. Rips and M. J. Hartmann, Phys. Rev. Lett. **110**, 120503 (2013).
[10] J. Moser, J. Güttinger, A. Eichler, M. J. Esplandiu, D. E. Liu, M. I. Dykman, and A. Bachtold, Nat. Nanotechnol. **8**, 493 (2013).
[11] P. Rabl, S. J. Kolkowitz, F. H. L. Koppens, J. G. E. Harris, P. Zoller, and M. D. Lukin, Nat. Phys. **6**, 602 (2010).
[12] S. E. Nigg, H. Paik, B. Vlastakis, G. Kirchmair, S. Shankar, L. Frunzio, M. H. Devoret, R. J. Schoelkopf, and S. M. Girvin, Phys. Rev. Lett. **108**, 240502 (2012).
[13] T. Ramos, V. Sudhir, K. Stannigel, P. Zoller, and T. J. Kippenberg, Phys. Rev. Lett. **110**, 193602 (2013).
[14] A. Jöckel, A. Faber, T. Kampschulte, M. Korppi, M. T. Rakher, and P. Treutlein, Nat. Nanotechnol. **10**, 55 (2015).
[15] J.-M. Pirkkalainen, S. U. Cho, F. Massel, J. Tuorila, T. T. Heikkilä, P. J. Hakonen, and M. A. Sillanpää, arXiv:1412.5518.
[16] M. Pechal, L. Huthmacher, C. Eichler, S. Zeytinoğlu, A. A. Abdumalikov, Jr., S. Berger, A. Wallraff, and S. Filipp, Phys. Rev. X **4**, 041010 (2014).
[17] J. Majer, J. M. Chow, J. M. Gambetta, J. Koch, B. R. Johnson, J. A. Schreier, L. Frunzio, D. I. Schuster, A. A. Houck, A. Wallraff, A. Blais, M. H. Devoret, S. M. Girvin, and R. J. Schoelkopf, Nature (London) **449**, 443 (2007).
[18] M. Hofheinz, E. M. Weig, M. Ansmann, R. C. Bialczak, E. Lucero, M. Neeley, A. D. O'Connell, H. Wang, J. M. Martinis, and A. N. Cleland, Nature (London) **454**, 310 (2008).
[19] M. V. Gustafsson, T. Aref, A. F. Kockum, M. K. Ekström, G. Johansson, and P. Delsing, Science **346**, 207 (2014).
[20] J.-M. Pirkkalainen, S. U. Cho, J. Li, G. S. Paraoanu, P. J. Hakonen, and M. A. Sillanpää, Nature (London) **494**, 211 (2013).
[21] T. T. Heikkilä, F. Massel, J. Tuorila, R. Khan, and M. A. Sillanpää, Phys. Rev. Lett. **112**, 203603 (2014).
[22] A. J. Rimberg, M. P. Blencowe, A. D. Armour, and P. D. Nation, New J. Phys. **16**, 055008 (2014).
[23] See the Supplemental Material at http://link.aps.org/supplemental/10.1103/PhysRevLett.114.173602 for a derivation of the Hamiltonian, details of the polaritonic description of the system, and more information about the state preparation protocols.
[24] R. Barends, J. Kelly, A. Megrant, D. Sank, E. Jeffrey, Y. Chen, Y. Yin, B. Chiaro, J. Mutus, C. Neill, P. O'Malley, P. Roushan, J. Wenner, T. C. White, A. N. Cleland, and J. M. Martinis, Phys. Rev. Lett. **111**, 080502 (2013).
[25] H. Paik, D. I. Schuster, L. S. Bishop, G. Kirchmair, G. Catelani, A. P. Sears, B. R. Johnson, M. J. Reagor, L. Frunzio, L. I. Glazman, S. M. Girvin, M. H. Devoret, and R. J. Schoelkopf, Phys. Rev. Lett. **107**, 240501 (2011).
[26] C. Rigetti, J. M. Gambetta, S. Poletto, B. L. T. Plourde, J. M. Chow, A. D. Córcoles, J. A. Smolin, S. T. Merkel, J. R. Rozen, G. A. Keefe, M. B. Rothwell, M. B. Ketchen, and M. Steffen, Phys. Rev. B **86**, 100506 (2012).
[27] N. Lörch and K. Hammerer, arXiv:1502.04112.
[28] J. D. Teufel, T. Donner, D. Li, J. W. Harlow, M. S. Allman, K. Cicak, A. J. Sirois, J. D. Whittaker, K. W. Lehnert, and R. W. Simmonds, Nature (London) **475**, 359 (2011).
[29] P. Rabl, Phys. Rev. B **82**, 165320 (2010).
[30] C. A. Regal, J. D. Teufel, and K. W. Lehnert, Nat. Phys. **4**, 555 (2008).
[31] X. Zhou, F. Hocke, A. Schliesser, A. Marx, H. Huebl, R. Gross, and T. J. Kippenberg, Nat. Phys. **9**, 179 (2013).
[32] M. Pernpeintner, T. Faust, F. Hocke, J. P. Kotthaus, E. M. Weig, H. Huebl, and R. Gross, Appl. Phys. Lett. **105**, 123106 (2014).
[33] A. Nunnenkamp, K. Børkje, and S. M. Girvin, Phys. Rev. A **85**, 051803 (2012).
[34] M. Steffen, J. M. Martinis, and I. L. Chuang, Phys. Rev. B **68**, 224518 (2003).
[35] K. Geerlings, Z. Leghtas, I. M. Pop, S. Shankar, L. Frunzio, R. J. Schoelkopf, M. Mirrahimi, and M. H. Devoret, Phys. Rev. Lett. **110**, 120501 (2013).
[36] D. M. Greenberger, M. A. Horne, and A. Zeilinger, *Bell's Theorem, Quantum Theory, and Conceptions of the Universe*, (Springer, Dordrecht, The Netherlands, 1989), pp. 69–72.
[37] L. Tian, Phys. Rev. B **72**, 195411 (2005).
[38] A. Asadian, C. Brukner, and P. Rabl, Phys. Rev. Lett. **112**, 190402 (2014).
[39] C. C. Gerry, Phys. Rev. A **54**, R2529 (1996).
[40] M. Hofheinz, H. Wang, M. Ansmann, R. C. Bialczak, E. Lucero, M. Neeley, A. D. O'Connell, D. Sank, J. Wenner, J. M. Martinis, and A. N. Cleland, Nature (London) **459**, 546 (2009).